This paper is published as part of a PCCP Themed Issue on:
Solid-State NMR Spectroscopy

Guest Editors: Paul Hodgkinson, Durham, UK, and Stephen Wimperis, Glasgow, UK

Editorial

Solid-State NMR Spectroscopy
Phys. Chem. Chem. Phys., 2009, **DOI:** 10.1039/b914008p

Perspectives

Recent advances in solid-state NMR spectroscopy of spin *I* = 1/2 nuclei
Anne Lesage, *Phys. Chem. Chem. Phys.*, 2009
DOI: 10.1039/b907733m

Recent advances in solid-state NMR spectroscopy of quadrupolar nuclei
Sharon E. Ashbrook, *Phys. Chem. Chem. Phys.*, 2009,
DOI: 10.1039/b907183k

Papers

Solid-state ^{17}O NMR as a sensitive probe of keto and *gem*-diol forms of α-keto acid derivatives
Jianfeng Zhu, Amanda J. Geris and Gang Wu, *Phys. Chem. Chem. Phys.*, 2009, **DOI:** 10.1039/b906438a

Anomalous resonances in ^{29}Si and ^{27}Al NMR spectra of pyrope ($[Mg,Fe]_3Al_2Si_3O_{12}$) garnets: effects of paramagnetic cations
Jonathan F. Stebbins and Kimberly E. Kelsey, *Phys. Chem. Chem. Phys.*, 2009, **DOI:** 10.1039/b904731j

New opportunities in acquisition and analysis of natural abundance complex solid-state ^{33}S MAS NMR spectra: $(CH_3NH_3)_2WS_4$
Hans J. Jakobsen, Henrik Bildsøe, Jørgen Skibsted, Michael Brorson, Bikshandarkoil R. Srinivasan, Christian Näther and Wolfgang Bensch, *Phys. Chem. Chem. Phys.*, 2009,
DOI: 10.1039/b904841n

An analytic expression for the double quantum ^{1}H nuclear magnetic resonance build-up and decay from a Gaussian polymer chain with dynamics governed by a single relaxation time
Michael E. Ries and Michael G. Brereton, *Phys. Chem. Chem. Phys.*, 2009, **DOI:** 10.1039/b905350f

Static solid-state ^{14}N NMR and computational studies of nitrogen EFG tensors in some crystalline amino acids
Luke A. O'Dell and Robert W. Schurko, *Phys. Chem. Chem. Phys.*, 2009, **DOI:** 10.1039/b906114b

Solid state deuteron relaxation time anisotropy measured with multiple echo acquisition
Robert L. Vold, Gina L. Hoatson, Liliya Vugmeyster, Dmitry Ostrovsky and Peter J. De Castro, *Phys. Chem. Chem. Phys.*, 2009, **DOI:** 10.1039/b907343d

Application of multinuclear magnetic resonance and gauge-including projector-augmented-wave calculations to the study of solid group 13 chlorides
Rebecca P. Chapman and David L. Bryce, *Phys. Chem. Chem. Phys.*, 2009, **DOI:** 10.1039/b906627f

High-resolution ^{17}O double-rotation NMR characterization of ring and non-ring oxygen in vitreous B_2O_3
Alan Wong, Andy P. Howes, Ben Parkinson, Tiit Anupõld, Ago Samoson, Diane Holland and Ray Dupree, *Phys. Chem. Chem. Phys.*, 2009, **DOI:** 10.1039/b906501f

Probing chemical disorder in glasses using silicon-29 NMR spectral editing
Julien Hiet, Michaël Deschamps, Nadia Pellerin, Franck Fayon and Dominique Massiot, *Phys. Chem. Chem. Phys.*, 2009,
DOI: 10.1039/b906399d

GIPAW (gauge including projected augmented wave) and local dynamics in ^{13}C and ^{29}Si solid state NMR: the study case of silsesquioxanes $(RSiO_{1.5})_8$
Christel Gervais, Laure Bonhomme-Coury, Francesco Mauri, Florence Babonneau and Christian Bonhomme, *Phys. Chem. Chem. Phys.*, 2009
DOI: 10.1039/b907450c

Determining relative proton–proton proximities from the build-up of two-dimensional correlation peaks in ^{1}H double-quantum MAS NMR: insight from multi-spin density-matrix simulations
Jonathan P. Bradley, Carmen Tripon, Claudiu Filip and Steven P. Brown, *Phys. Chem. Chem. Phys.*, 2009
DOI: 10.1039/b906400a

Manifestation of Landau level effects in optically-pumped NMR of semi-insulating GaAs
Stacy Mui, Kannan Ramaswamy, Christopher J. Stanton, Scott A. Crooker and Sophia E. Hayes, *Phys. Chem. Chem. Phys.*, 2009
DOI: 10.1039/b907588g

Motional heterogeneity in single-site silica-supported species revealed by deuteron NMR
Julia Gath, Gina L. Hoaston, Robert L. Vold, Romain Berthoud, Christophe Copéret, Mary Grellier, Sylviane Sabo-Etienne, Anne Lesage and Lyndon Emsley, *Phys. Chem. Chem. Phys.*, 2009
DOI: 10.1039/b907665d

Magnesium silicate dissolution investigated by ^{29}Si MAS, ^{1}H–^{29}Si CPMAS, ^{25}Mg QCPMG, and ^{1}H–^{25}Mg CP QCPMG NMR
Michael C. Davis, William J. Brouwer, David J. Wesolowski, Lawrence M. Anovitz, Andrew S. Lipton and Karl T. Mueller, *Phys. Chem. Chem. Phys.*, 2009
DOI: 10.1039/b907494e

Intermediate motions and dipolar couplings as studied by Lee–Goldburg cross-polarization NMR: Hartmann–Hahn matching profiles
Marcio Fernando Cobo, Kateřina Maliňáková, Detlef Reichert, Kay Saalwächter and Eduardo Ribeiro deAzevedo, *Phys. Chem. Chem. Phys.*, 2009
DOI: 10.1039/b907674c

Measurements of relative chemical shift tensor orientations in solid-state NMR: new slow magic angle spinning dipolar recoupling experiments
Andrew P. S. Jurd and Jeremy J. Titman, *Phys. Chem. Chem. Phys.*, 2009
DOI: 10.1039/b906814g

Signal loss in 1D magic-angle spinning exchange NMR (CODEX): radio-frequency limitations and intermediate motions
Christiane Hackel, Cornelius Franz, Anja Achilles, Kay Saalwächter and Detlef Reichert, *Phys. Chem. Chem. Phys.*, 2009
DOI: 10.1039/b906527j

Calculation of fluorine chemical shift tensors for the interpretation of oriented ^{19}F-NMR spectra of gramicidin A in membranes
Ulrich Sternberg, Marco Klipfel, Stephan L. Grage, Raiker Witter and Anne S. Ulrich, *Phys. Chem. Chem. Phys.*, 2009
DOI: 10.1039/b908236k

***J*-Based 3D sidechain correlation in solid-state proteins**
Ye Tian, Lingling Chen, Dimitri Niks, J. Michael Kaiser, Jinfeng Lai, Chad M. Rienstra, Michael F. Dunn and Leonard J. Mueller, *Phys. Chem. Chem. Phys.*, 2009
DOI: 10.1039/b911570f

Natural abundance ^{13}C and ^{15}N solid-state NMR analysis of paramagnetic transition-metal cyanide coordination polymers
Pedro M. Aguiar, Michael J. Katz, Daniel B. Leznoff and Scott Kroeker, *Phys. Chem. Chem. Phys.*, 2009
DOI: 10.1039/b907747b

Signal loss in 1D magic-angle spinning exchange NMR (CODEX): radio-frequency limitations and intermediate motions

Christiane Hackel, Cornelius Franz, Anja Achilles, Kay Saalwächter* and Detlef Reichert*

Received 1st April 2009, Accepted 2nd July 2009
First published as an Advance Article on the web 17th July 2009
DOI: 10.1039/b906527j

The popular 1D MAS exchange experiment CODEX suffers limitations due to signal loss during the finite recoupling periods, during which the magnetization evolves in the transverse plane. Here, we address the origins and possible improvements of this problem, aimed at (i) an optimization of the signal-to-noise ratio in the experiments, as well as harnessing intermediate-motion induced signal loss for obtaining approximate information on (ii) correlation times and (iii) potential distributions, where the latter are often found in polymeric systems. First, we show that the intensity of the signal is sensitive to the radiofrequency (rf) parameters of the carbon recoupling and proton decoupling, and care must be taken to gain optimal signal intensity. Optimum conditions are found for recoupling pulses being as short as possible for large chemical shift anisotropy (CSA) values, and approaching a ratio of 3 between the nutation frequencies for protonated carbons, calling for an individual adjustment in each case. Second, we demonstrate that the effect of intermediate motions can be studied semi-quantitatively by combining CODEX data with its constant-time modification CONTRA, which allows for a tuning of the signal loss due to intermediate motions. Third, for the case of samples featuring a distribution of correlation times, we propose a procedure to obtain an estimate of the proportion of molecular segments in the sample for which the CODEX data are representative, *i.e.*, which share of segments moves truly in the slow-motion regime. The procedure involves the combination of CODEX data with a cross-polarisation (CP) reference experiment for an estimate of the full sample magnetization; it is demonstrated on the example of semi-crystalline poly(ethylene oxide).

Introduction

Dynamic processes play an important role for the properties of materials. In particular in organic solids such as polymers and proteins, slow motions are directly related to mechanical[1] or transport properties.[2] Solid-state magic-angle spinning (MAS) exchange experiments have proved to be among the most efficient experimental approaches[3–5] and among them, the centerband-only detection of exchange (CODEX) sequence[6] is perhaps the most often applied pulse experiment. CODEX relies on the detection of molecular reorientations by their effect on the orientation-dependent resonance frequency, which is governed by an anisotropic NMR interaction, for example the chemical shift anisotropy (CSA). Since the experiment is performed under MAS, a recoupling of the CSA is necessary to achieve a measurable effect on the experimental data. See Fig. 1 for the pulse sequence.

After an initial recoupling period, during which an orientation-dependent phase is picked up, the nucleus might change its orientation during the subsequent mixing period, t_m, and, as a result, a different phase is acquired in the second recoupling period. This leads to a signal decay that directly indicates the presence of a molecular reorientation. The CSA recoupling is performed by trains of rotor-synchronized π pulses, in analogy to the REDOR experiment used for heteronuclear recoupling.[7] CODEX is convenient, as it only

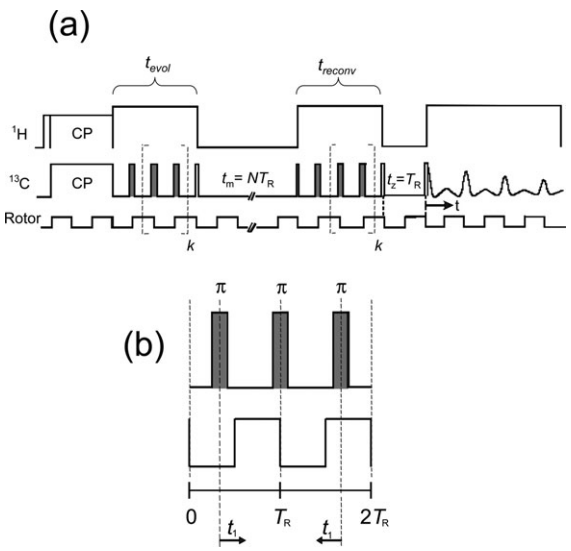

Fig. 1 (a) Pulse sequence of the CODEX 1D MAS exchange experiment. (b) Scheme of the basic recoupling cycle for the CONTRA experiment, resulting in a t_1-dependent scaling of the CSA recoupling. For details, see ref. 8.

University of Halle, Department of Physics, Betty-Heimann-Strasse 7, 06120 Halle, Germany. E-mail: kay.saalwaechter@physik.uni-halle.de, detlef.reichert@physik.uni-halle.de

requires the acquisition of two 1D spectra per time point (mixing time or recoupling time, see below), resulting in significant time savings as compared to 2D exchange NMR,[3] and is thus applicable to natural isotopic abundance samples. Both the correlation time of motion, τ_c, as well as the amplitude of the molecular reorientation can be determined from separate sets of 1D experiments. The correlation time can, in principle, be extracted from the decay of the signal intensity *vs.* the length of t_m, while the latter must be determined from the comparison of the decay as a function of the CSA recoupling time, measured in multiples of rotor cycles, NT_R, with calculations based on model assumptions.

The experiment is commonly run in a normalized fashion such that a normalized signal S/S_0 is constructed, which involves the acquisition of two spectra with swapped t_m and final *z*-filter time (t_z), which automatically compensates for T_1 effects during t_m. The normalized signal, S/S_0, takes values between 1 (no exchange; $t_m \ll \tau_c$) and 0 (isotropic motion in full exchange; $t_m \gg \tau_c$). The value of the plateau for S/S_0 ($t_m \gg \tau_c$) is indicative of the number of inequivalent sites, M, that the molecule can visit during the molecular reorientation, $S/S_0(t_m \gg \tau_c) = 1/M$, but must be corrected in case of the presence of a fraction of signal related to immobile or fast-limit mobile molecules.

There are some problems associated with this experiment which we will address in this paper. They are related to the obvious issue of optimizing for maximum signal intensity, which is mainly due to potential signal decay during the recoupling cycles (apparent T_2^{RC}), which is always a matter of concern in long pulse sequences. Optimizing for long T_2^{RC} is highly desirable but not always possible. The relaxation during the CSA recoupling cycles may be related to incomplete ^1H–^{13}C decoupling during the free-precession periods between the π pulses, as well as to imperfect π pulses and/or interference of the ^{13}C pulses with the ^1H decoupling irradiation. It can be optimized by a number of measures, in addition to the obvious attention to efficient ^1H decoupling during recoupling, as was already mentioned early on for the conceptually similar REDOR experiments.[7]

There are additional contributions to the apparent T_2^{RC} decay, however, that are related to the molecular dynamics of the material. The experiment is most sensitive to the desired dynamic information when τ_c is on the order of the accessible t_m, *i.e.* when the entire signal decay $S/S_0 = 1 \rightarrow S/S_0 = 1/M$ occurs within a range extending from the length of one rotor cycle, T_R, up to a value on the order of T_1. These limits define the so-called "slow-motion regime" for which the experiment was designed to work. If the process is too slow (and we are putting aside effects of spin diffusion[9]), the dynamic process is outside of the dynamic window of the method. Then, the S/S_0 *vs.* t_m curve is constant at $S/S_0 = 1$ and the dynamic process remains undetected. On the other hand, the shortest possible value of the rotor-synchronized mixing period t_m is naturally 1 T_R, which, for typical MAS spinning speeds, is on the order of 100 μs. If τ_c is on this order (*i.e.* the motion is in the so-called intermediate motional regime), molecular reorientations already occur during the CSA recoupling cycles, rendering the precession frequency not only dependent on the MAS rotation but also on the dynamic process, leading to more complex S/S_0 *vs.* t_m curves.[10] In particular, there is additional dephasing (similar to the well-known "dynamic broadening") during the recoupling cycles that is not refocused by the π pulses, leading to signal loss, and also invalidating the relation $S/S_0(t_m \gg \tau_c) = 1/M$, putting aside for the moment the issue of additional immobile segments.

The situation becomes particularly complex when dynamic processes with a wide distribution of correlation times are involved. This essentially leads to a combined effect of the above-mentioned regimes. In particular, it means that parts of the sample signal which are in the intermediate regime are selectively suppressed during the recoupling cycles. Correlation time distributions are common for polymeric materials, and the question arises how conclusions drawn from the experimental data are representative for the investigated sample, *i.e.* whether the acquired CODEX signal represents all molecules in the sample, or whether a share of the signal arising from more mobile parts has already decayed during the recoupling cycles and is thus suppressed to a certain extent in the data. Though intermediate-regime motions might already manifest themselves in dynamic line broadening by increased line widths in the NMR spectrum, in polymeric systems, with intrinsically broad lines, it is difficult to identify the presence of such a problem by mere inspection of the spectrum and, thus, one needs to resort to procedures such as the one proposed below.

The present paper is focused on the problems introduced above: (i) how to minimize the decay due to T_2^{RC} for best signal-to-noise ratio, (ii) how to estimate correlation times that are too short to be reliably measured by t_m-dependent S/S_0 curves, and (iii) how to estimate for the case of τ_c distributions the share of signal that—for a given length of the recoupling periods—has already escaped detection by intermediate-regime motions and does not contribute to the measured intensity data. We present systematic experimental investigations of the effects of the ^{13}C nutation frequency and ^{13}C–^1H dipolar couplings during the π pulses, and propose approaches based on constant-time and reference experiments in order to quantify signal loss due to intermediate motions and correlation time distributions.

Experimental

The NMR experiments were performed on a BRUKER AVANCE II spectrometer at ^1H and ^{13}C frequencies of 400.16 and 100.6 MHz, respectively, with a standard BRUKER 4 mm MAS probe. ^1H CW and SPINAL64 decoupling was used during the recoupling and acquisition periods, respectively. The ^1H nutation frequency was 78 kHz. Natural-abundance glycine and dimethyl sulfone (DMS) were obtained from Sigma-Aldrich and used without further treatment. As a material that exhibits a distribution of correlation times, we choose semi-crystalline Poly(ethylene oxide), PEO.[11] The sample was kindly provided by Prof. Thurn-Albrecht, University of Halle. The sample with a molecular weight of 280 kDa was isothermally crystallized at 320 K. The dynamic process under observation is the helical jump motion of the polymer chains in the crystallites,[13] which is a fairly well-defined process through the defined 7_2 helical structure

of the crystals. The helix is distorted, however,[12] and the time constant of the motion features a substantial distribution.[13]

Results and discussion

Signal loss due to finite π pulses

Fig. 1a shows the sequence of the CODEX experiment. To extract τ_c, the length of t_m is incremented, and the resulting decay *vs.* t_m is fitted to an appropriate function; in simple cases to an exponential decay, and for the case of τ_c distributions, for instance, to a stretched exponential, $\exp\{-(t_m/\tau_c)^{\beta}\}$. On the other hand, to determine the amplitude motion, the length of the CSA recoupling cycles, NT_R, $N = 2(k + 1)$ being the total number of recoupling cycles, is incremented. The experiment is commonly performed in a normalized fashion, *i.e.* by two subsequent experiments: the normalization or reference experiment with negligible t_m (*i.e.* usually one rotor cycle), resulting in the signal $S_0(NT_R, t_z)$, is sensitive to signal decay due to T_2^{RC} during NT_R, T_1 decay during the final z storage period t_z, and signal loss due to imperfect pulses. On the other hand, the actual exchange experiment results in the signal $S(NT_R, t_m)$, which is additionally sensitive to slow motional processes that occur during t_m. For the two experiments, identical T_1 relaxation effects can be achieved by setting t_m of the exchange experiment equal to t_z of the reference experiment (*i.e.*, the two delays are simply interchanged). The effect of the different motional regimes on the final signal intensity can be roughly factorized as

$$S(NT_R, t_m) = f^{int}(NT_R)\exp\left(-\frac{NT_R}{T_2^{RC}}\right)f^{slow}(t_m)\exp\left(-\frac{t_m}{T_1}\right)$$

$$S_0(NT_R, t_z) = f^{int}(NT_R)\exp\left(-\frac{NT_R}{T_2^{RC}}\right)\exp\left(-\frac{t_z}{T_1}\right), \quad (1)$$

where f^{slow} and f^{int} are the signal decays due to slow and intermediate-regime motions during the mixing period and the recoupling cycles, respectively. From now on, we identify dynamic effects during recoupling only with the latter quantity, and subsume in T_2^{RC} all radiofrequency (rf)- and decoupling-related effects to be addressed in this section. Taking the ratio of the two data sets results in the signal S/S_0, which is essentially free from any relaxation contributions and contains only the information about the slow dynamic process,

$$\frac{S(NT_R, t_m)}{S_0(NT_R, t_z)} = f^{slow}(t_m), \quad (2)$$

when t_z of the reference experiment equals t_m.

We will now address the issue of reasonably large T_2^{RC} and focus first on the question whether incomplete ^{1}H decoupling or effects of the π pulses have the most significant effect. We applied the CODEX sequence to glycine, a molecule that does not exhibit any dynamic process in either the slow or the intermediate motional regimes. For our considerations, it is sufficient to run the S_0 experiment only, for it is most sensitive to the effects we are after. Fig. 2a shows the $S_0(NT_R)$ for the CH_2 resonance of natural-abundance glycine for MAS rates of

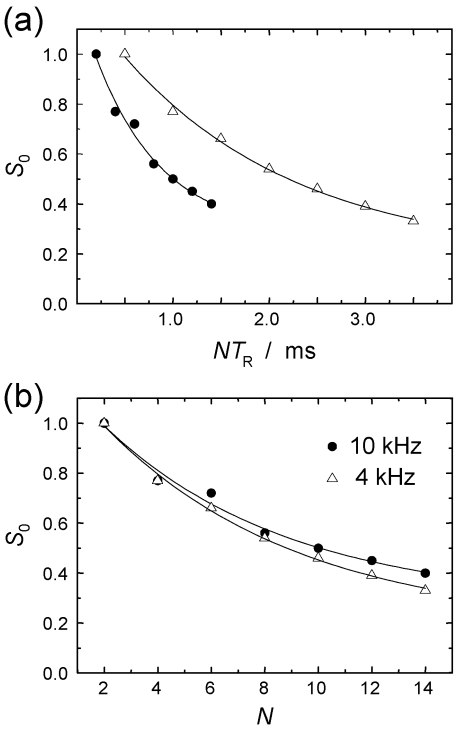

Fig. 2 CODEX S_0 signal for the CH_2 group of glycine for 10 (●) and 4 kHz (△) dependent on (a) NT_R and (b) N, *i.e.*, the total number of recoupling cycles.

4 and 10 kHz; the time constant of the decay is T_2^{RC}. It shows a faster signal decay *vs.* NT_R for the faster MAS rate, however, this information is not sufficient to separate the two effects. To do so, we plotted the data *vs.* the number of recoupling cycles (N) only, shown in Fig. 2b, and here the two data sets almost coincide, clearly indicating that the main contribution to the decay has little dependence on the length of the free precession period, *i.e.* does not arise from incomplete ^{1}H decoupling but from effects of the π pulses only. Two more observations support this finding: first, the small difference between the two curves in Fig. 2b favors faster spinning, which leads to better averaging of the ^{1}H–^{13}C dipolar coupling, which is intuitive. Second, we performed additional experiments, replacing the CW by TPPM decoupling during the recoupling cycles. There was no difference between these experiments beyond the margin of error, supporting our assumption that the details of the ^{1}H decoupling do not significantly affect T_2^{RC} in this case.

Since it is now clear that the main effect for a shortening of T_2^{RC} in a rigid sample is mainly an effect of the π pulses, we will now explore its origin. First, note that a finite length of the pulses does not challenge the recoupling efficiency *per se*; this effect can be easily accounted for using a (surprisingly small) scaling factor.[14] There are two obvious reasons for the finite-length effect on S_0, namely potential problems related to a finite excitation bandwidth and resonance offsets,[7] or cross polarization (CP)-type effects, arising upon simultaneous irradiation of both ^{1}H and ^{13}C in a wide range of rf conditions. Though the length of the pulses is typically as short as a few microseconds, the transfer of polarization can be rather efficient, leading to substantial alterations of the ^{13}C

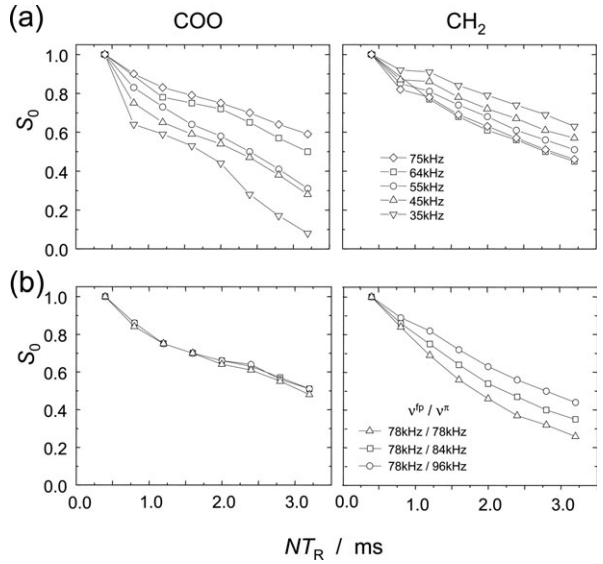

Fig. 3 CODEX signal S_0 *vs.* NT_R for the COO (left) and CH_2 (right) groups of glycine. The MAS spinning speed is 5 kHz. (a) Dependence on the ^{13}C nutation frequencies, *i.e.* length of the π pulses. (b) Dependence on the ^1H nutation (decoupling) frequencies during the free precession periods, $\nu_{^1H}^{fp}$ and during the π pulses, $\nu_{^1H}^{\pi}$, of the recoupling cycles.

magnetization. To distinguish the two effects, we turn to experiments in which the nutation frequency of the carbon pulses, $\nu_{^{13}C}$, is reduced, thus (i) lengthening the π pulses and (ii) moving farther away from the Hartmann–Hahn condition and its spinning sidebands.

Glycine is again a reasonable test substance, for the COO group exhibits a large CSA and is thus sensitive to rf offsets, while it is insensitive to dipolar effects owing to the large distance to the nearest proton. In contrast, the strongly proton-coupled CH_2 group is a good indicator for carbon–proton dipolar effects. Fig. 3a shows data from both groups at a MAS rate of 5 kHz. We observe an opposite effect on the COO and CH_2 signals upon increasing $\nu_{^{13}C}$: while the T_2^{RC} for COO shortens with longer π pulses (clearly an off-resonance effect), T_2^{RC} for CH_2 increases for longer pulses. The latter might appear counter-intuitive, however it is straightforwardly explained by a reduction of cross-polarization efficiency under increasingly mismatched Hartmann–Hahn conditions. As it was shown,[15] the ^1H–^{13}C cross-talk should become minimal if the ratio of the ^1H and ^{13}C nutation frequencies approaches 3, 5, 7,...

In order to better separate potentially combined effects of resonance offset and CP transfer for the CH_2 case, Fig. 3b shows data for which the length of the π pulses (and thus $\nu_{^{13}C}$) is kept constant and $\nu_{^1H}$ is increased during the pulses to establish an off-Hartmann–Hahn condition. Clearly, the COO data are not affected at all, while the CH_2 data show the expected improvement. However, the range of potential variation of $\nu_{^1H}/\nu_{^{13}C}$ is much smaller as compared to Fig. 3a, as an upper limit for $\nu_{^1H}$ is posed by the probe head. We also checked the effect of replacing the regular π pulses by composite pulses of the type $(\pi/2)_0(\pi)_{90}(\pi/2)_0$ in order to decrease the effect of the resonance offsets, however, the effect was rather disappointing, showing no improvement, neither for the COO resonance nor for the CH_2 (data not shown). The offset compensation is obviously balanced by the adverse effect of much-increased effective pulse length and potential CP-related loss.

A potentially interesting alternative to address the problems at hand could be the use of very fast MAS at rates beyond 60 kHz, where the ^1H–^1H homonuclear dipolar coupling is significantly decreased by MAS alone and low-power decoupling is an alternative.[16] This option would allow the combination of rather short ^{13}C pulses with a sufficiently large offset from the Hartmann–Hahn condition, and it should certainly be tested in the future. However, we note that the use of significantly smaller rotors and thus sample amounts is not fully offset by comparable filling factors of smaller coils, which challenges the signal-to-noise ratio achievable in reasonable time. Isotopic labelling is not always an option, as it significantly speeds up adverse spin diffusion effects among the heteronuclei. Note that CODEX experiments are intrinsically less sensitive than simple CP MAS spectra by a factor of at least 4, where intensity loss by a factor of 2 arises from the phase cycle that combines a separate *z*-storage of cos and sin components of the signal arising during the first recoupling period, and another factor of 2 related to the need to perform S_0 and S experiments, plus additional T_2^{RC} effects.

Signal loss due to intermediate motions

Now we turn to the second issue, namely the effect of intermediate motions on the overall signal, parametrized by $f^{int}(NT_R)$ in eqn (1). It is well known since the beginning of NMR that for motions with τ_c on the order of the rotor period, the interaction timescale in a MAS experiment, and thus the actual timescale of true T_2-type effects, lead to a rapid decay of the signal.[17,18] For a demonstration, we focus on DMS as a model substance for a well-studied molecular jump process,[10,19–21] where the two methyl groups exchange places in jumps around the C_2 axis, corresponding to a reorientation of the symmetry axis of its almost symmetric CSA tensor (δ = 37.3 ppm) by 108°. Decay curves of the S_0 reference signal are shown in Fig. 4a. Clearly, the decays become very pronounced upon entering a temperature range where the correlation times fall into the ms range and below. As shown earlier,[10] this decay is prominently due to the fact that the tensor undergoing the intermediate motions is recoupled.

The effect is, in principle, related to the conventional dynamic line broadening of MAS spectra, where the rotor echoes in free MAS evolution decay due to the loss of phase coherence picked up during the MAS. During one rotor cycle, the phase integrated over one rotor period averages back to zero (creating a rotor echo) only if the molecular segment does not change its orientation. Under recoupling conditions, the situation is aggravated in that the pick-up of phase coherence does not revert back to zero at the end of a single rotor cycle, but continues throughout a whole recoupling block. The echo formation of the S_0 experiment thus extends over a much longer timescale—in our case the "unwinding" of the acquired phase takes as long as the second recoupling period, which means that the experiment is much more sensitive to any motion occurring on this longer timescale.

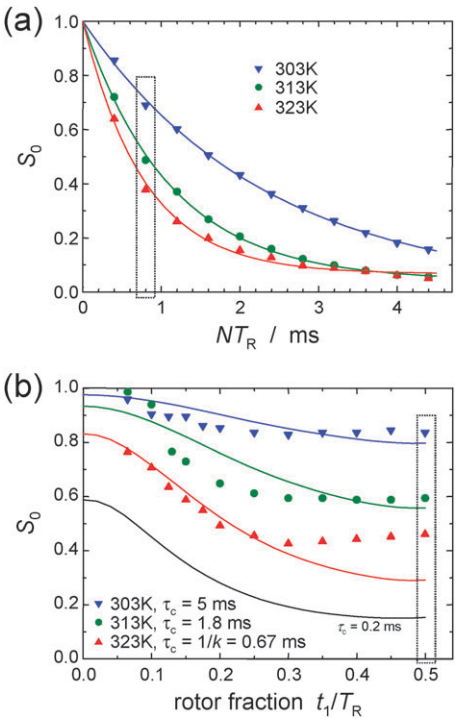

Fig. 4 (a) CODEX S_0 intensity decays of DMS at 5 kHz MAS as a function of the recoupling time for different temperatures, including exponential fits (see our previous work[10] for an explanation of the slight non-exponentiality observed at 323 K). (b) Corresponding CONTRA ($2 \times 2T_R$ = 0.8 ms recouping time) S_0 intensity traces as a function of π pulse placement time, t_1, highlighting the effect of recoupling on intensity loss. The dotted boxes in (a) and (b) mark equivalent data points for which the scaled relative intensities were kept fixed. The lines are theoretical predictions (see text), using correlation times and tensor parameters given in ref. 19 and 20

The strong decay has two consequences: firstly, that the sensitivity of the experiment is severely challenged when correlation times in this range are to be studied by CODEX with its finite recoupling time that determines its angular sensitivity (note that τ_c = 1 ms can in principle still be covered by short mixing times of a few T_R), and that the experimental results will be strongly biased in case the sample is heterogeneous (*vide infra*). In principle, the decay due to f^{int} can be harnessed for an extraction of the correlation time; however, as is clear from the previous section, other adverse effects such as rf-related imperfections need to be suitably accounted for. In our previous paper,[10] we suggested a reference experiment with nominally no recoupling by grouping together pairs of π pulses, which was subject to limitations for the reason that the finite pulse lengths do not permit a pulse timing that leads to truly zero recoupling—this would only be possible if all π pulses were delta pulses and could be placed at multiples of T_R. In this vein, "minimal recoupling" reference experiments have recently been proposed by Schmidt-Rohr and coworkers[22] in order to better normalize for the action of adverse T_1 relaxation effects during recoupling experiments involving dipolar couplings to quadrupolar spins (RIDER),[23] which in fact pose similar problems to the one at hand, *i.e.*, loss of phase coherence on the recoupling time scale.

An alternative is provided by continuous constant-time approaches, which were proposed as modifications of the basic CODEX. In the two experiments, S-CODEX[24] (scaled CODEX) and CONTRA[8] (constant-time recoupling of anisotropies), the recoupling of the CSA is controlled by changing the timing of the recoupling π pulses continuously rather than (or in addition to) changing the overall number of recoupling cycles. Such strategies have already been proposed in the earliest papers on the REDOR technique,[25] but, apparently, did not gain comparable popularity. Fig. 1b shows the basic cycle of the CONTRA experiment of length $2T_R$. The key point is that maximum (REDOR-type) recoupling is achieved when the recoupling pulse are placed at $t_1 = T_R/2$, while moving the two central π pulses towards the flanking π pulses placed at full rotor cycles, *i.e.* $t_1 \rightarrow 0$, the recoupling efficiency decreases and eventually approaches zero. In the original papers, this was used to investigate slow dynamic processes which feature a rapid decay *vs.* NT_R (large CSA values and/or large-amplitude reorientations) and would require very fast spinning for the conventional CODEX experiment in order to obtain information on the reorientation angle.

We here suggest the use of the CONTRA approach to obtain more information on intermediate-motional effects at constant level of rf-related signal decay. CONTRA differs from S-CODEX only in the little detail that, in the latter, the same two shifting pulses move into the same direction (positive t_1). While S-CODEX works with any number of recoupling cycles, the CONTRA experiment—being a mirror-symmetric experiment[25]—always requires an even number of cycles.[8] CONTRA proved less susceptible to experimental imperfections, and also features a more favorable tunability of the recoupling effect. Fig. 5 displays calculated S-CODEX and CONTRA dephasing curves (dashed/dotted lines) as compared to conventional CODEX. Full symbols in Fig. 5 should serve as examples for experimentally accessible data points (closer data spacing can of course realized by faster spinning). Such curves are usually used to estimate the

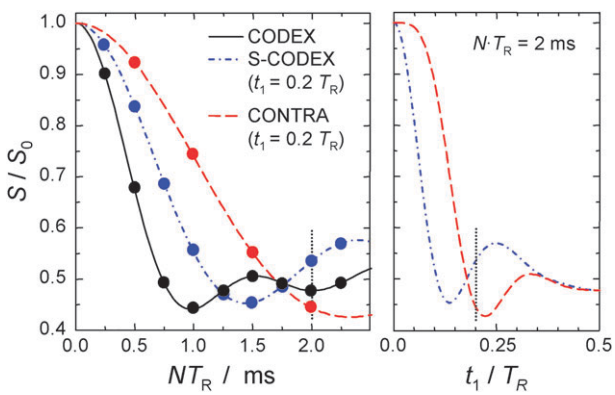

Fig. 5 Dephased intensity decay data (S) for CODEX, S-CODEX and CONTRA. The left part shows S/S_0 as a function of NT_R simulated for the case of DMS, where accessible data points for 8 kHz MAS are indicated. On the right, practically more feasible t_1 variations for constant 4 T_R recoupling are shown, which can be measured in continuous fashion, demonstrating the scaling effect on the recoupling efficiency. Dashed lines mark equivalent data points.

orientation angle, and it is easily appreciated that for fixed t_1 values, the scaled versions provide a larger number of meaningful data points, in particular when they are taken in constant-time mode (right part of Fig. 5). Note that the CONTRA t_1 dependence (tuned recoupling efficiency) is less steep, providing a better quantification of the behavior towards $t_1 \rightarrow 0$, which is needed to sample the full range of recoupling behaviours.

The approach to study intermediate-regime dynamics is now *not* to monitor the dephased signal S, but rather the reference signal S_0. In cases without intermediate motions, this signal would be constant and not a function of t_1. The data shown in Fig. 4b are thus a direct proof of the presence of dephasing due to intermediate motions. Note that the plotted data taken at different temperatures were adjusted relative to each other using the intensity ratios taken from Fig. 4a, where exponential extrapolations served to determine the initial intensities for $NT_R = 0$. We compare the experimental data with theoretical predictions based on the second-moment approximation (Anderson–Weiss theory).[26] In our previous work, we could show that different experiments, such as the DIPSHIFT experiment[27] or Lee–Goldburg CP,[28] when applied to samples with intermediate motions, can be conveniently described by the closed-form analytical expressions calculated on the basis of this approach with only little compromises, even when the investigated dynamics are a finite-site jump process rather than the assumed continuous rotational diffusion. Analytical approximations for the CONTRA signal in combination with motion can be obtained from Hirschinger's result for the signal in a MAS experiment after N refocusing (π) pulses,[26]

$$G(t>\tau_N) = \exp\left\{ \begin{array}{c} M_2^{\mathrm{HT}}\left[\frac{2}{3}F_N(0,\omega_r,t) + \frac{1}{3}F_N(0,2\omega_\mathrm{r},t)\right] \\ +\Delta M_2\left[\frac{2}{3}F_N(\Gamma,\omega_\mathrm{r},t) + \frac{1}{3}F_N(\Gamma,2\omega_\mathrm{r},t)\right] \end{array} \right\}, \tag{3}$$

where

$$F_N(\Gamma, n\omega_\mathrm{r}, t) = \frac{1}{\Gamma^2 + n^2\omega_\mathrm{r}^2}\left\{ \begin{array}{c} 2\sum_{j=1}^{N}(-1)^j[h^{(n)}(\tau_j) - (-1)^N h^{(n)}(t-\tau_j)] \\ +4\sum_{j=1}^{N}\sum_{k>j}^{N}(-1)^{k-j}h^{(n)}(\tau_k - \tau_j) \\ -(-1)^N h^{(n)}(t) + (2N+1)\frac{\Gamma^2 - n^2\omega_\mathrm{r}^2}{\Gamma^2 + n^2\omega_\mathrm{r}^2} - \Gamma t \end{array} \right\}, \tag{4}$$

$$h^{(n)}(t) = \frac{\exp(-\Gamma t)}{\Gamma^2 + n^2\omega_\mathrm{r}^2}[(\Gamma^2 - n^2\omega_\mathrm{r}^2)\cos(n\omega_\mathrm{r}t) - 2\Gamma n\omega_\mathrm{r}\sin(n\omega_\mathrm{r}t)], \tag{5}$$

$$\Delta M_2 = M_2^{\mathrm{LT}} - M_2^{\mathrm{HT}} \tag{6}$$

and $\Gamma = 1/\tau_\mathrm{c}$. The τ_i denote the timings of the N π pulses, and t is the time at which detection starts. In order to use this result for the CONTRA S_0 experiment, we simply omit the mixing time and the two $\pi/2$ storage and read-out pulses before and after the experimentally necessary minimum, t_m of $1T_\mathrm{R}$. This introduces a small systematic error, yet a proper account of the finite mixing time would necessitate the derivation of a new equation, which is beyond the scope of this report. For the case of CSA (in analogy to the case of heteronuclear dipolar couplings), the low-temperature (static) and high-temperature (fast-limit) second moments are $M_2^{\mathrm{LT}} \approx \frac{1}{5}\delta^2 \approx 1.14 \times 10^8$ (rad s^{-1})^2 and $M_2^{\mathrm{HT}} = S^2 M_2^{\mathrm{LT}}$, with an order parameter $S \approx 0.32$, which we calculated numerically from the second moment of the fast-limit averaged ($\eta \approx 1$) CSA tensor of DMS based on the parameters given in ref. 19.

The analytical results in Fig. 4b are based on correlation times calculated from the Arrhenius parameters published in ref. 20, and are thus predictions without free parameters rather than fits. It is observed that the experimental trends are overall reproduced by the theory. Note in particular that there is still a decay for the initial values at $t_1 = 0$ corresponding to the decay in a perfect "no-recoupling" reference experiment, which is identical to the decay of the rotor echoes in free MAS time evolution. Discrepancies are observed for the intensities at larger values of t_1 approaching $T_\mathrm{R}/2$. We have previously observed that results based on the second-moment approximation (assuming a Gaussian rather than a Pake-type frequency distribution) deviate, in particular for longer times (higher accumulated phase),[27] and we also stress that the process at hand is a two-site jump rather than the assumed diffusion on a cone. The clarification of the origin of the discrepancies is deferred to future work, which will also involve explicit density matrix simulations. For the moment, we conclude that observing variations in the (fully refocused) S_0 reference signal of CONTRA-type experiments holds promise as a tool to study correlation times in the intermediate regime; however, we point out that the original CONTRA experiment, with its separate storage of cos and sin parts of the transverse coherence during t_m is certainly not the most efficient experiment. Omitting the $\pi/2$ pulses and t_m in the actual experiment, leading to the recoupled-echo experiment proposed in ref. 10, is a better strategy that we will follow in future work. With the present results, we mainly highlight the signal loss effects in CODEX experiments, which are most problematic for heterogeneous samples.

CODEX on samples with correlation time distributions

As already mentioned, the presence of a τ_c distribution may severely bias the results that can be obtained from fits to conventional CODEX t_m dependences. It is thus mandatory to estimate the share of molecules in the sample which actually contribute to the CODEX signal, *i.e.* to quantify the unavoidable signal loss due to intermediate motions. This means, for our case, that dynamic heterogeneities in the sample that cause a distribution of τ_c lead to nonuniform $f^{\mathrm{int}}(NT_\mathrm{R})$, which, in turn, results in a non-representative sampling of differently mobile segments and their proportional representation in the final intensity data after a given NT_R. We note that, in principle, such arguments also hold for CP and all other experiments relying on polarization enhancement *via* dipolar couplings, which thus act as a dynamic filter, suppressing the

signals from molecules which are in the intermediate regime.[27] However, recent work showed that CP-related bias effects in exchange experiments are not dramatic,[28–30] provided that reasonable CP times on the order of a few 100 μs are used. This provides sufficient transfer even in fast-limit averaged cases (provided that the motion is anisotropic), but avoids large bias effects due to $T_{1\rho}$ effects that typically occur on a longer timescale than the intermediate-motional effects in coherent transfer experiments.[28]

We demonstrate this effect on the example of PEO. Fig. 6a shows a CODEX mixing-time dependence, where it is seen that only a stretched exponential function with $\beta = 0.7$ fits the data reasonably well. This value indicates a correlation time distribution over more then one decade. In fact, recent static ^{2}H stimulated-echo experiments[13] even indicate β around 0.5, suggesting an even wider distribution (note that static stimulated-echo experiments suffer similar bias problems to CODEX, but a smaller bias due to a comparably shorter evolution delay is expected).

Clearly, as schematically depicted in Fig. 6b, a significant part of the sample signal is not detected in CODEX for this temperature. A low-τ_c wing of the distribution may in fact already yield some signal from fast-limit-averaged segments (with again increased f^{int}), which contribute equally to the S and S_0 experiments. This explains why the intensity plateau f_∞ does not reach the value of 1/7 expected for a 7-site jump of the sevenfold PEO helix (an estimate based on the results below indicates that the "wrong" plateau can be explained by an initial ~5% contribution from fast-limit segments). An alternative explanation would of course be a fraction of fully immobile helices, as suggested by Vogel.[13] Note that the crystallinity of the sample is larger than 80%, and that the signal of mobile amorphous parts is efficiently suppressed by the CP[11,12] due to small couplings and rather short $T_{1\rho}$. We neglect the (small) fast-limit or rigid contributions and now focus on the largely suppressed signal fraction with τ_c in the intermediate regime as compared to the remaining slow-motion fraction, using the decay of the S_0 experiment as an indicator.

Fig. 7a first compares the $S_0(NT_R)$ decay for the CH_2 groups of PEO at 243 K with the CH_2 signal of glycine measured under identical conditions. Note the choice of the identical CH_x groups (with similar ^{1}H–^{13}C heteronuclear dipolar couplings) permits a direct comparison between the different samples. While the decay for glycine is only caused by the rf-related effects described above ($\sim T_2^{RC}$), the decay for PEO is much stronger, immediately identifying a substantial

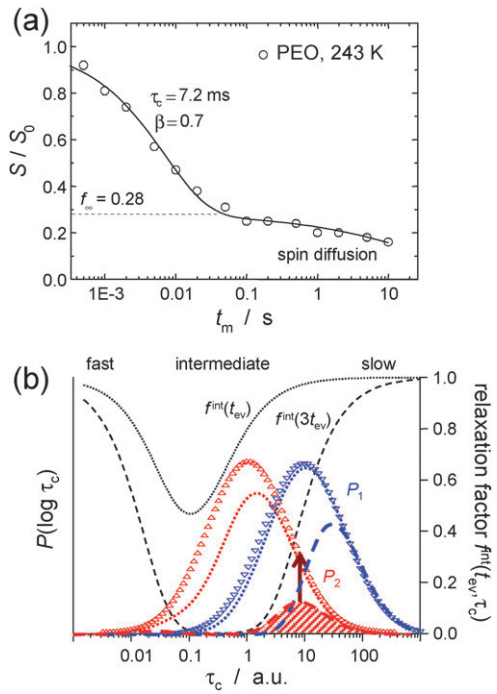

Fig. 6 (a) CODEX S/S_0 mixing time dependence for PEO at 243 K, measured at 10 kHz MAS and $NT_R = 1.2$ ms. The decay was fitted to a double stretched exponential, with the second component being associated with spin diffusion effects. The helical-jump process (first component) is described by a correlation time of 7.2 ms with a stretching exponent of 0.7 and an intensity plateau at $S/S_0 = 0.28$. (b) Scheme demonstrating the effect of correlation-time dependent damping factors (f^{int}) for different evolution delays on the overall signal of a sample with a heterogeneous distribution of correlation times ($P(\log \tau_c)$, triangles, with P_2 representing a higher temperature). The dotted and dashed lines below the corresponding initial distributions are the products of $P(\log \tau_c)$ with the corresponding f^{int} functions; the hatched area and the arrow represent the singly-exponential back extrapolation as discussed in the text.

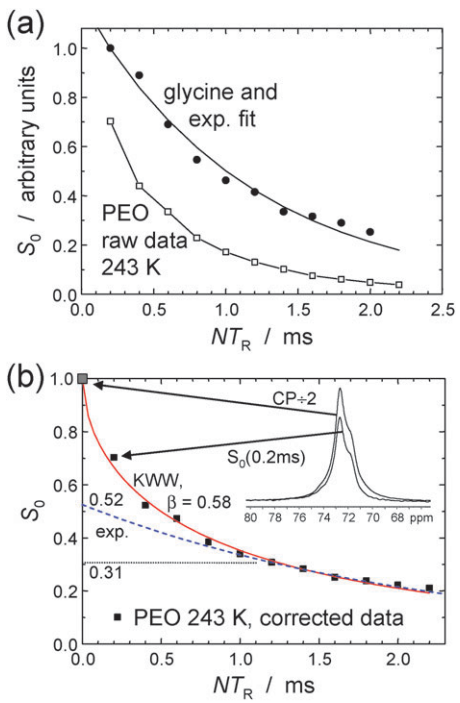

Fig. 7 CODEX S_0 intensity decays as a function of NT_R at 10 kHz MAS and 243 K. (a) As-measured raw data for PEO and glycine, with an exponential fit to the latter yielding T_2^{RC}. (b) Processed PEO data obtained by division through T_2^{RC} decay correcting for rf limitations and Kohlrausch–Williams–Watts (KWW) fit indicating the distribution effect ($\beta = 0.58$). The inset shows a spectrum corresponding to the first S_0 data point and a 50%-scaled CP spectrum representing the full sample signal. The signal loss due to intermediate motions can then be quantified, possibly by singly exponential back-extrapolation to obtain an upper-limit estimate.

decay due to intermediate motions ($\sim f^{\mathrm{int}}$). To separate the two effects, we fitted the $S_0(NT_R)$ data for glycine by an exponential function and divided the $S_0(NT_R)$ for PEO by this function. The results are shown in Fig. 7b, where it must be noted that a back correction to $NT_R = 0$ in analogy to Fig. 5a, which would be needed to estimate the overall sample intensity (given by the area under the original distribution curves in Fig. 6b) is not feasible. This is because the decay is also strongly stretched, immediately suggesting distribution effects. Fitting the data as-is yields an exponent β of around 0.35, inflicting a large error on the back-extrapolation.

Therefore, the initial intensity must be determined from a separate CP reference experiment without recoupling cycles. The inset in Fig. 7b shows a comparison of the S_0 experiment with the shortest possible recoupling time and the corresponding CP spectrum. The latter needs to be scaled by a factor of 0.5, taking into account the storage of cos and sin components in separate transients, which halves the sensitivity of the CODEX experiment. The fine structure of the CH_2 line in PEO is explained by the distorted helical structure, and was rigorously assigned in ref. 12. Note that the S_0 spectrum is slightly better resolved, which is an indication for selective loss of domains with unfavourable correlation times (their signal being broadened due to interferences between motion and the decoupling).

Using the data point provided by the integral of the CP spectrum allows for a much improved stretched-exponential fit of the S_0 decay, which now gives a stretching exponent of 0.58, which is in better agreement with the value given by Vogel *et al.*[13] This value is lower than the one obtained from the t_m-dependent fit in Fig. 6a, which is trivially explained by the fact that the residual signal after a recoupling time of 1.2 ms characterizes only a fraction of the original distribution (see Fig. 6b), and, thus, is apparently narrower.

With the well-defined initial point, the signal remaining after 1.2 ms recoupling is now quantitatively determined to be 31% of the overall sample signal (assuming no bias due to the initial CP). Of course, the slow-motion wing of the original distribution shown in Fig. 6b has a larger area than this value, because the parts remaining for the CODEX t_m analysis have decayed partially during the recoupling. Tentatively, one may assume that the remaining distribution is narrow enough to be described by a single exponential $f^{\mathrm{int}}(NT_R)$. Then, a few data points starting at 1.2 ms recoupling time can be fitted and back-extrapolated with a single exponential, giving 52% as an upper limit of the sample fraction characterized by the CODEX t_m decay. An up-correction in this range is indicated by the arrow in Fig. 6b. Clearly, the two numbers (31 and 52%) would not differ if the $f^{\mathrm{int}}(\tau_c)$ damping term was a 1-step function, completely suppressing only segments with a given maximum, $\tau_c^{\max}$, and retaining full signal above. The two numbers were, on the other hand, directly meaningful if the f^{int} were 0 below and a constant <1 above $\tau_c^{\max}$ over the value range of $P(\log \tau_c)$. In this way, the two numbers provide a range of sample fractions that ultimately characterize the distribution width.

Functions f^{int} describing the signal loss may also be estimated on the basis of Andersen–Weiss theory and our future work is devoted to the development of strategies that yield quantitative information on width and shape of correlation time distributions. Finally, note that the first step of the procedure, *i.e.* the removal of the rf-contribution to obtain the true f^{int}-decay using the glycine reference data, is essential in this case. Approaches using CONTRA-type constant-time experiments may, on the other hand, prove useful to characterize sub-populations that remain after given evolution times.

Conclusion

We have presented investigations aimed at an improved understanding and a reduction of the signal loss in the popular 1D-MAS exchange experiment CODEX. We have addressed (i) the optimization of the signal-to-noise ratio in the experiments, as well as harnessing intermediate-motion induced signal loss for obtaining approximate information on (ii) correlation times and (iii) potential distributions, where the latter are often found in polymeric systems.

We have shown that the intensity of the signal is very sensitive to the rf parameters of the carbon recoupling pulses and the proton decoupling, and care must be taken to set them to optimal values. While it is common knowledge that pulses should be as short as possible, *i.e.* to have the nutation frequencies as large as possible, cases of strongly ^{1}H-coupled carbons might favour the opposite, *i.e.* to reduce the carbon nutation frequency and thus, to lengthen the pulses. Optimum conditions are found for recoupling pulses being as short as possible for large CSA values, and approaching a ratio of 3 between the nutation frequencies for protonated carbons, calling for an individual adjustment in each case.

Second, we have demonstrated that the effect of intermediate motions can be studied semi-quantitatively by combining CODEX S_0 reference intensity decay data with its constant-time modification CONTRA, which allows for a tuning of the signal loss due to intermediate motions. The presence of intermediate-regime dynamics is immediately apparent from the experimental data, providing an easy means to check whether such dynamics are present. This is particularly easy since the necessary experimental data (the reference intensities S_0) are normally acquired anyway for the characterization of slow motions, which is the typical application of CODEX/CONTRA experiments. A comparison of the data with an analytical function derived from a second-moment approach (Anderson–Weiss theory) even allows for a semi-quantitative estimate of the correlation time.

Third, for the case of samples featuring a distribution of correlation times, demonstrated on the example of the helical-jump process in the crystallites of semi-crystalline poly(ethylene oxide), we have proposed a procedure to obtain an estimate of the proportion of molecular segments in the sample for which CODEX data are representative, *i.e.*, which share of segments moves truly in the slow-motion regime. The procedure involves the combination of CODEX S_0 decay data with a CP reference experiment under identical conditions for an estimate of the full sample magnetization at zero recoupling time. The overall decay is typically strongly stretched when a substantial distribution is present, and can be fitted reliably only when the zero-time point is measured rather than

determined by extrapolation. A stretched exponential fit to the decay then provides a stretching exponent, β, that characterizes the width of the correlation time distribution. CODEX mixing-time dependencies using a given recoupling time are therefore typical only for a fraction of the sample that has not decayed due to intermediate motions. A lower limit of this fraction is immediately given by the value of the normalized S_0 decay curve, and an upper-limit estimate may be obtained by a singly exponential back-extrapolation based on S_0 decay data at around the given recoupling time. With these strategies, we hope to have provided information that may enable a further widespread use of the valuable MAS exchange experiment CODEX.

Acknowledgements

This work was supported by the Deutsche Forschungsgemeinschaft (DFG) in the framework of the grants SFB 418 and RE 1025/16. Significant investments into our NMR infrastructure from the European Regional Development Fund (ERDF) by the European Union are also gratefully acknowledged.

References

1 W. G. Hu and K. Schmidt-Rohr, *Acta Polym.*, 1999, **50**, 271.
2 N. C. Mello, T. J. Bonagamba, H. Panepucci, K. Dahmouche, P. Judeinstein and M. A. Aegerter, *Macromolecules*, 2000, **33**, 1280.
3 K. Schmidt-Rohr and H. W. Spiess, *Multidimensional Solid-State NMR and Polymers*, Academic Press, London, 1994.
4 E. R. deAzevedo, T. J. Bonagamba and D. Reichert, *Prog. Nucl. Magn. Reson. Spectrosc.*, 2005, **47**, 137.
5 Z. Luz, P. Tekely and D. Reichert, *Prog. Nucl. Magn. Reson. Spectrosc.*, 2002, **41**, 83.
6 E. R. deAzevedo, W. G. Hu, T. J. Bonagamba and K. Schmidt-Rohr, *J. Am. Chem. Soc.*, 1999, **121**, 8411.
7 T. Gullion, *Concepts Magn. Reson.*, 1998, **10**, 277.
8 D. Reichert, O. Pascui, T. J. Bonagamba, P. Belton, A. Schmidt and E. R. deAzevedo, *J. Magn. Reson.*, 2008, **191**, 141.
9 D. Reichert, T. J. Bonagamba and K. Schmidt-Rohr, *J. Magn. Reson.*, 2001, **151**, 129.
10 K. Saalwächter and I. Fischbach, *J. Magn. Reson.*, 2002, **157**, 17.
11 A. Johansson and J. Tegenfeldt, *Macromolecules*, 1992, **25**, 4712.
12 D. J. Harris, T. J. Bonagamba, M. Hong and K. Schmidt-Rohr, *Polymer*, 2005, **46**, 11737.
13 M. Vogel, C. Herbers and B. Koch, *J. Phys. Chem. B*, 2008, **112**, 11217.
14 C. P. Jaroniec, B. A. Tounge, C. M. Rienstra, J. Herzfeld and R. G. Griffin, *J. Magn. Reson.*, 2000, **146**, 132.
15 Y. Ishii, J. Ashida and T. Terao, *Chem. Phys. Lett.*, 1995, **246**, 439.
16 M. Ernst, A. Samoson and B. H. Meier, *Chem. Phys. Lett.*, 2001, **348**, 293.
17 H. S. Gutowsky and C. H. Holm, *J. Chem. Phys.*, 1956, **25**, 1228.
18 E. L. Hahn and D. E. Maxwell, *Phys. Rev.*, 1952, **88**, 1070.
19 M. S. Solum, K. W. Zilm, J. Michl and D. M. Grant, *J. Phys. Chem.*, 1983, **87**, 2940.
20 D. E. Favre, D. J. Schaefer and B. F. Chmelka, *J. Magn. Reson.*, 1998, **134**, 261.
21 D. Reichert, G. Hempel, H. Zimmermann, H. Schneider and Z. Luz, *Solid State Nucl. Magn. Reson.*, 2000, **18**, 17.
22 Y. Y. Hu and K. Schmidt-Rohr, *J. Magn. Reson.*, 2009, **197**, 193.
23 K. Saalwächter and K. Schmidt-Rohr, *J. Magn. Reson.*, 2000, **145**, 161.
24 D. Reichert, O. Pascui, T. J. Bonagamba, E. R. deAzevedo and A. Schmidt, *Chem. Phys. Lett.*, 2003, **380**, 583.
25 T. Gullion and J. Schaefer, *Adv. Magn. Reson.*, 1989, **13**, 57.
26 J. Hirschinger, *Solid State Nucl. Magn. Reson.*, 2008, **34**, 210.
27 E. R. deAzevedo, K. Saalwächter, O. Pascui, A. A. De Souza, T. J. Bonagamba and D. Reichert, *J. Chem. Phys.*, 2008, **128**, 104505.
28 M. F. Cobo, K. Malinakova, D. Reichert, K. Saalwächter and E. deAzevedo, *Phys. Chem. Chem. Phys.*, 2009, DOI: 10.1039/b907674c.
29 M. Wachowicz, L. Gill and J. L. White, *Macromolecules*, 2009, **42**, 553.
30 D. Reichert and K. Saalwächter, in *Encyclopedia of Magnetic Resonance*, ed. R. K. Harris and R. Wasylishen, John Wiley, Chichester, 2008, DOI: 10.1002/9780470034590.emrstm1020.

